

# Enabling Multiple Access for Non-Line-of-Sight Light-to-Camera Communications

Fan Yang, Shining Li, Zhe Yang, *Member, IEEE*, Tao Gu, *Senior Member, IEEE*, and Cheng Qian

**Abstract**—Light-to-Camera Communication (LCC) has emerged as a new wireless communication technology with great potential to benefit a broad range of applications. However, the existing LCC systems either require the camera directly facing to the lights or can only communicate over a single link, resulting in low throughputs and being fragile to ambient illuminant interference. We present HYCACO, a novel LCC system, which enables multiple light emitting diodes (LEDs) with an unaltered camera to communicate via the non-line-of-sight (NLoS) links. Different from other NLoS LCC systems, the proposed scheme is resilient to the complex indoor luminous environment. HYCACO can decode the messages by exploring the mixed reflected optical signals transmitted from multiple LEDs. By further exploiting the rolling shutter mechanism, we present the optimal optical frequencies and camera exposure duration selection strategy to achieve the best performance. We built a hardware prototype to demonstrate the efficiency of the proposed scheme under different application scenarios. The experimental results show that the system throughput reaches 4.5 Kbps on iPhone 6s. With the robustness, improved system throughput and ease of use, HYCACO has great potentials to be used in a wide range of applications such as advertising, tagging objects, and device certifications.

**Index Terms**—Visible Light Communication, Camera Communication, Rolling Shutter, LED, NLoS, Smartphone.



## 1 INTRODUCTION

IN recent years, the rolling shutter based visible light communication (VLC) has been a promising technique which uses the Complementary Metal-Oxide-Semiconductor (CMOS) sensor within a digital camera for data reception. It enables the camera to sample optical signals at a much faster rate than the frame rate, and can utilize the pervasively deployed commercial off-the-shelf (COTS) LEDs as transmitters. Since most of the COTS smartphones have CMOS cameras built-in, LCC has shown great potential in data transmission to overcome the crowded radio spectrum. Furthermore, LCC has some unique features, e.g., it provides a natural way to visually associate the received information with the transmitter's identity, which can be used in indoor localization, augmented reality, etc.

LCC can be classified into two categories. One is line-of-sight (LoS), i.e., the camera directly faces to the LED [1]. The other one is non-line-of-sight (NLoS), i.e., the camera observes the reflected optical signals [2], as illustrated in Fig. 1. However, each of the kinds has hit its bottleneck of throughput. The throughput depends on several factors including the signal frequency and the camera features, mostly importantly on the region of interest (RoI) [3]. The NLoS LCC typically has higher throughput because the optical signals occupy the whole image, while the optical signals only occupy part of the image via the LoS link unless the camera is very close to the LED. However, the received signal strength (RSS) of a NLoS link is attenuated significantly due to the diffuse reflection, which increases

the demodulation error. Moreover, optical signals from other illuminants are mixed by the reflector, which causes significant interferences.

Utilizing multiple LEDs for NLoS LCC is challenging for four main reasons: (i) The information transmitted from each LED is very difficult, if not impossible, to be extracted because the entire image is filled by the mixed reflected optical signals. (ii) The captured optical signals are mixed with the environment background and substantial noise introduced by camera hardwares (e.g., heterogeneity of color pixels, salt-and-pepper noise). (iii) Paramount to the practical implementation of LCC is ensuring high-quality lighting that is satisfactory to human. (iv) LCC is a one-way communication link, via which the transmitter cannot get any feedback from the receiver. It brings the intrinsic difficulties to implement the unsynchronized communication in real time.

In this paper, we propose a HYbrid light-to-CAMERA Communication (HYCACO) system. Different from many existing approaches, HYCACO works in a more realistic indoor luminous environments (i.e., multiple light sources and natural illumination), where multiple LEDs are coordinated to emit square wave signals simultaneously. We embed the information in the phase of the square waves, which is called phase-shift keying (PSK). Different from the conventional PSK, we propose a new scheme, hybrid PSK (HPSK), where different subcarriers adopt different orders of PSKs. Therefore, the received signals can be considered as a combination of square waveforms with different properties, e.g., phase and/or frequency. In particular, when a CMOS camera obtains an image with respect to the reflector illuminated by the LEDs, it contains bright and dark bands corresponding to the mixed optical signals. In order to extract information from the mixed signals, we propose a SUPERimposed Rect-wave Division (SURD) algorithm.

- F. Yang, C. Qian, S. Li and Z. Yang are with the School of Computer Science and Engineering, Northwestern Polytechnical University, Xi'an China, 710129. E-mail: {craftsman, infinite}@mail.nwpu.edu.cn, {lishining, zyang}@nwpu.edu.cn.
- T. Gu is with School of Computer Science and IT, RMIT University, Australia. Email: tao.gu@rmit.edu.au

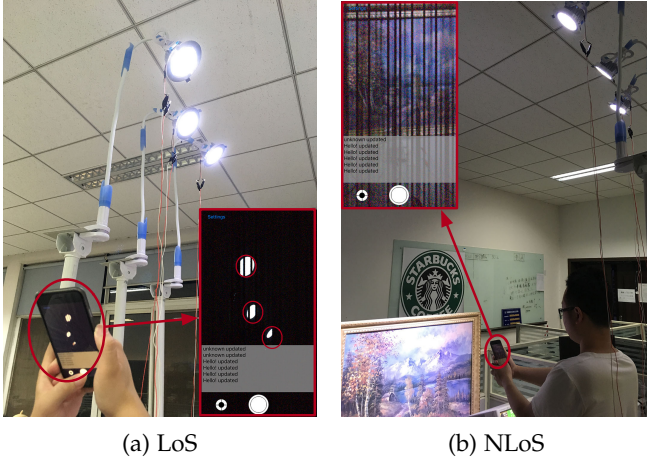


Fig. 1: Comparison between LoS and NLoS light-to-camera communications.

We further exploit the rolling shutter effect and figure out the relationship between the camera settings and the features of optical signals. We propose a solution to recover the optical signal by capturing two images with different exposure durations but the same exposure value (EV). We use a simple preamble to help to sample hundreds of judging points from millions of pixels in the image. Thus, HYCACO is high computational efficiency and can provide realtime responses with the COTS smartphones. Besides, We address the symbol loss problem, which is caused by the unsynchronized communication channel, with the Luby transform codes (LT codes) [4].

We have implemented a prototype system to evaluate the performance of HYCACO. We employ an Arduino UNO board to act the modulator to control up to 7 LEDs as the transmitter. At the receiver end, we develop an iOS application and an Android application to verify the performance using iPhone 6s and Nexus 5, respectively. We conduct the extensive experiments under various camera settings and environments to evaluate the system performance comprehensively. The experimental results have demonstrated the efficacy of the proposed scheme.

In summary, this paper makes the following contributions:

- To our knowledge, HYCACO is the first NLoS LCC system which enables multiple access. We have implemented a prototype system and test the performance of HYCACO in different scenarios. The extensive experimental results demonstrate that HYCACO can achieve a throughput of  $4.5Kbps$ . This is a significant improvement compared with other state-of-the-art LCC systems.
- We propose a new modulation scheme, HPSK, to transmit messages from multiple LEDs and also propose the corresponding algorithm, SURD, to demodulate the signals.
- We first present the relationship between the camera settings and the features of optical signals, and come out with the optimal optical frequency and camera exposure duration selection strategy.
- We propose a simple solution to separate the captured

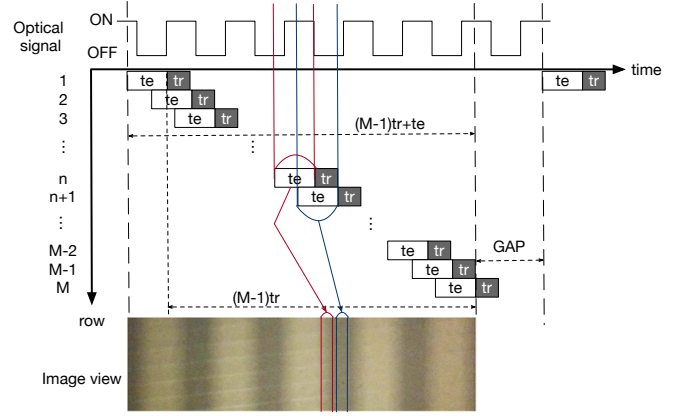


Fig. 2: The optical signal is a square wave.  $t_e$  is the exposure duration of the captured image and  $t_r$  is the readout duration of the camera.

optical signals from the complex image background, which improves the robustness of the LCC systems.

## 2 PRELIMINARY & SYSTEM ARCHITECTURE

Before presenting the proposed HYCACO scheme, we present the preliminary results about rolling shutter cameras and describe other physical constraints on the transmission of the optical channel introduced into the current mainstream LED and digital camera techniques.

### 2.1 Image Capture Model

The electronic rolling shutters have been widely employed by most of the smartphones which have CMOS cameras built-in. When a CMOS camera captures photos or videos, it does not expose every pixel of the entire image all at once. Instead, each sensor array of pixels in the image is triggered by row (shown in Fig. 2). The exposure duration of a pixel row is shifted by a fixed amount of readout duration  $t_r$ . It means that a pulsing light will illuminate only some rows of the pixels at a time, resulting in the alternately dark and bright bands in the image. We can detect the frequency of these bands in the image, and thus infer the frequency of the pulsing light. Therefore, it can act as a sampling process to the optical signal with much higher sampling rate than the frame rate of the camera. As a result, this effect allows us to record the flicker pattern by taking spatio-temporal images with an unaltered digital camera, where different patterns can be used to represent different symbols.

Conceptually, the image captured by the camera can be thought of as having two layers: the texture layer and the signal layer. HYCACO consists of several ON-OFF keying (OOK) modulated LEDs as the transmitters and a CMOS sensor as the receiver. The luminance emitted from an LED is  $L$ , and the state of the LED is controlled by the function  $f_i(t)$ , where  $i$  denotes the serial number of the LED. When the LED is ON,  $f_i(t) = 1$ ; otherwise,  $f_i(t) = 0$ . Thus, the illuminance of light falling on the camera is

$$e(t) = E + \sum H_i(0)Lf_i(t), \quad (1)$$

where  $H_i(0)$  is the channel DC gain [5] and  $E$  is the non-flickering lights (such as sunlight). Let  $r(x, y, t)$  be the

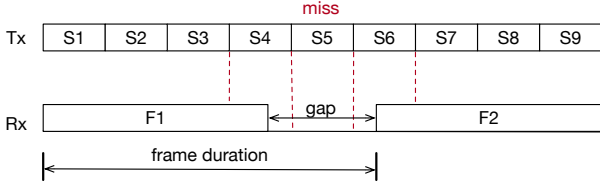


Fig. 3: Mixed symbol and symbol loss due to unsynchronization.

radiance incident at sensor pixel  $(x, y)$  at time  $t$ . The radiance  $r(x, y, t)$  can be factorized into spatial and temporal components:

$$r(x, y, t) = l(x, y)e(t), \quad (2)$$

where  $l(x, y)$  is the amplitude of the temporal radiance profile at pixel  $(x, y)$  and is determined by the image background. The measured brightness value of a pixel at  $(x, y)$  in the image is

$$\begin{aligned} i(x, y) &= k l(x, y) \int_{-\infty}^{\infty} s(t_y - t)e(t)dt + n(x, y), \\ &= \underbrace{k l(x, y)}_{\text{texture layer}} \times \underbrace{(s * e)(t_y)}_{\text{signal layer}} + n(x, y), \end{aligned} \quad (3)$$

where  $k$  is the sensor gain,  $s(t_y - t)$  is the shutter function [6],  $t_y$  is the temporal shift for a pixel in row  $y$ , and  $n(x, y)$  is the image noise. Since the signal layer is unidimensional, we perform analysis on vertical sum images—that is,  $i(y) = \sum_x i(x, y)$ ,  $l(y) = \sum_x l(x, y)$  and  $n(y) = \sum_x n(x, y) = 0$ , because the image noises follow a Gaussian distribution. Then, Equation (3) can be written as

$$i(y) = k l(y) \times (s * e)(t_y). \quad (4)$$

## 2.2 Unsynchronized LCC Channel

The characteristic of a camera's discontinuous receiving and the diversity of cameras lead to an unsynchronized LCC channel. Such an unsynchronized communication channel is very likely to experience the mixed symbol frame and the symbol loss problems. RollingLight [1] demonstrates these problems under different unsynchronized scenarios. The optical signals emitted from the LEDs are continuous, but the camera receives the signals frame by frame. A camera does not expose at all time in a frame duration. There exists a time gap between the end time of the exposure of the last row and the start time of the next frame, as illustrated in Fig. 2.

For example, as shown in Fig. 3, there exists a time gap between the end of exposure in frame  $F1$  and the start of exposure in frame  $F2$ . Frame  $F1$  receives a mixture of symbol  $S1, S2, S3$ , and part of  $S4$ . When the length of the gap is longer than the symbol duration, some symbols may be completely lost, e.g., symbol  $S5$ . In this case, symbol  $S4, S5, S6$  will not be extracted by the receiver. Different frame rates cause different levels of unsynchronizations, which lead to different symbol loss ratios [7].

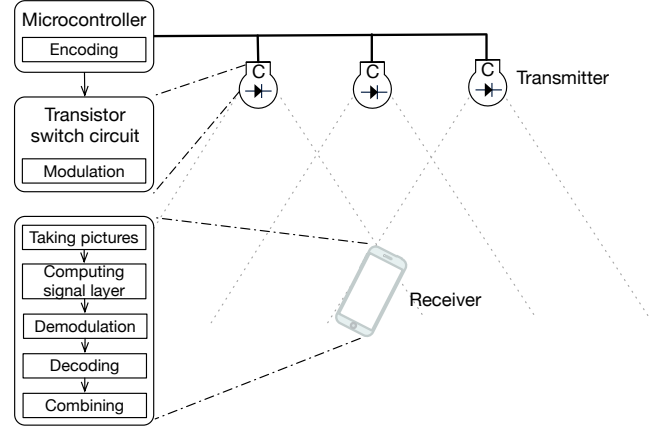


Fig. 4: Shows the architecture of HYCACO. The transmitter is several temporally modulated LEDs, and the receiver is a rolling shutter camera.

## 2.3 System Architecture

The architecture of HYCACO is shown in Fig. 4. Several COTS LEDs connected to transistor switch circuits are employed as the transmitter. A microcontroller encodes the input data to ON-OFF symbols and dispatches the symbols to the circuits. Thus, the data waveforms are modulated onto the instantaneous power of the optical carriers. A smartphone with a built-in CMOS camera is employed as the receiver. First, the smartphone continuously takes images of the reflector and calculates the signal layer of each image. Second, the signal layers are demodulated to several sequences of N-ary symbols according to the number of LEDs. Third, we decode the symbol sequences to binary data packets. Finally, we combine the data packets to retrieve the full input message.

## 3 CARRIER FREQUENCY SELECTION

Without loss of generality, we assume that LCC is used for both lighting and communication. Hence, the LEDs used in the LCC system should meet the lighting requirements for human. When the carrier frequency is smaller than eye's temporal resolution, called critical flicker frequency (CFF), flicker happens [8]. Typically, human eyes are able to resolve up to 50Hz to luminance flicker and 25Hz to chromatic flicker [9]. Although human eye has a cutoff frequency in the vicinity of 50Hz, some studies have shown that long-term exposure to higher frequency (unintentional) flickering (in the 70 to 160 Hz range) can also cause malaise, headaches, and visual impairment [10]. Besides, the perceived brightness of an LED varies proportionally to the average duty cycle of its flicker pattern. Therefore, the duty cycle in a CFF cycle duration should be unchanged too.

The biggest Advantage of NLoS LCC is it can easily amplify the RoI to the full width of the receiver. As illustrated in Fig. 2, the camera captures an image with an exposure duration  $t_e$ . Let  $M$  denote the width (number of pixel rows) of the image. The duration for the imager to open and allow photons to enter is  $(M - 1)t_r + t_e$ . However, the signal layer of the image is the convolution of the shutter function and the optical signal. Hence the duration of the signal recorded in the image is  $(M - 1)t_r$ .

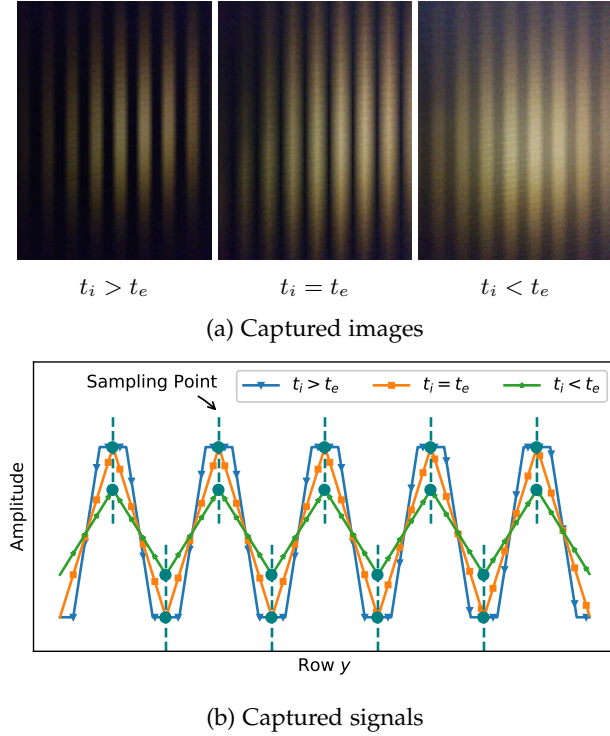


Fig. 5: The gradient of brightness changes due to the rolling shutter effect.  $t_i$  is the pulse duration, and  $t_e$  is the exposure duration.

For most cameras of smartphones, the shutter function can be considered as a rect window function, and the window length is the exposure duration. Under the same pulsing LED, images captured with different exposure durations would result in different stripe patterns, as shown in Fig. 5a. The brightnesses across the bright and dark bands change gradually, though this may not be obvious to the naked eyes. The capturing can be classified into three circumstances according to the relationship of the pulse duration  $t_i$  and the exposure duration  $t_e$ , i.e.,  $t_i > t_e$ ,  $t_i = t_e$ , and  $t_i < t_e$ . The simulated signal layers of the images in Fig. 5a are illustrated in Fig. 5b. As we can see, as long as  $t_i \geq t_e$ , there exists a set of sample points in the signal layer that can fully describe the optical signal.

Furthermore, there are some physical constraints of cameras placed on the reception of the optical signal. Cameras on the market usually have different  $t_r$ . We propose a simple method to calibrate  $t_r$  by sending a known preamble. We measure several phones'  $t_r$  and the supported range of exposure duration. We find  $t_r$  is much smaller than the minimum exposure duration.  $t_r$  is from several microseconds to a dozen microseconds. Theoretically, the range of the carrier frequency can be from 160 to  $1/2t_r$  Hz. However, when  $t_i < t_e$ , we cannot infer complete spatial detail of the carrier from the signal layer. In our proposal, HYCACO needs both the spatial and temporal detail of the carriers to perform the demodulation. Thus, we set  $t_i = t_e$  to obtain the maximum achievable throughput.

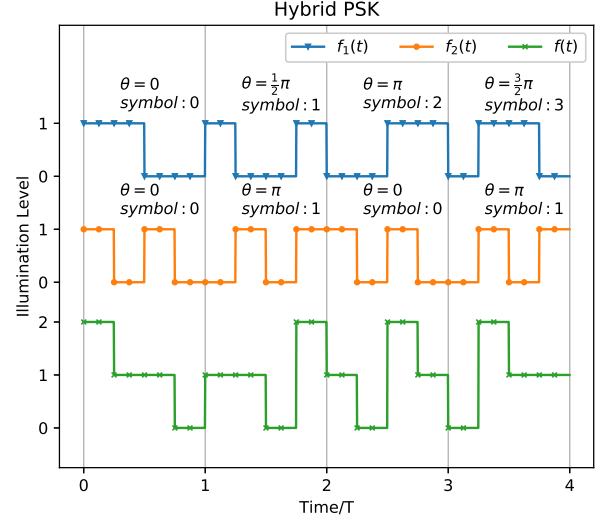


Fig. 6: Shows a HPSK modulation example, where  $symbol$  is a N-ary number and N is the order of PSK.  $f$  is the sum of  $f_1$  and  $f_2$ . The numbers on the Y-axis represent the perceived illumination levels, e.g., 0 means all the LEDs are off.

## 4 HYCACO DESIGN

### 4.1 Modulation and Encoding Scheme with Multiple Access

The inspiration of our modulation scheme comes from Orthogonal Frequency Division Multiplexing (OFDM). The frequency waveform emitted from each LED can be seemed as a subcarrier. Thus, the optical carrier is

$$f(t) = \sum f_i(t), \quad (5)$$

where  $f_i$  is the  $i^{th}$  subcarrier. In our prototypes, the transmitters share the same controller and are thus inherently synchronized. By decoding the messages modulated on each subcarrier, the receiver can communicate with each transmitter, respectively. For the convenience of evaluation, we let each transmitter sends a piece of input data, and the receiver combines the pieces to retrieve the full input data.

In this paper, a HPSK modulation scheme is proposed. Each subcarrier is modulated with a certain order of PSK. The distinct orders depend on the frequency and the symbol duration  $T$  (we use the pulse duration  $t_i$  as the time unit, denoted by 1). The frequency of subcarrier  $f_i$  is  $i/T$  and it adopts  $T/i$  order of PSK, as illustrated in Fig. 6. Subcarrier  $f_i$  can be expressed as follows:

$$f_i(t) = \begin{cases} 1, & \frac{nT}{i} - \frac{S_i}{T} \leq t < \frac{nT}{i} - \frac{S_i}{T} + \frac{T}{2i} \\ 0, & \frac{nT}{i} - \frac{S_i}{T} + \frac{T}{2i} \leq t < \frac{nT}{i} - \frac{S_i}{T} + \frac{T}{i} \end{cases}, \quad (6)$$

where  $S_i$  denotes the symbol it represents, and  $n = 0, 1, 2, \dots, i-1$ .

First of all, we need to choose the minimum symbol duration  $T$  according to the number of transmitters. The subcarrier frequency  $i/T$  has the following constraints:

- The frequency range of the subcarriers is from 160 to  $1/2t_i$  Hz.
- $i \in \mathbb{N}$ , where  $\mathbb{N}$  denotes natural numbers.

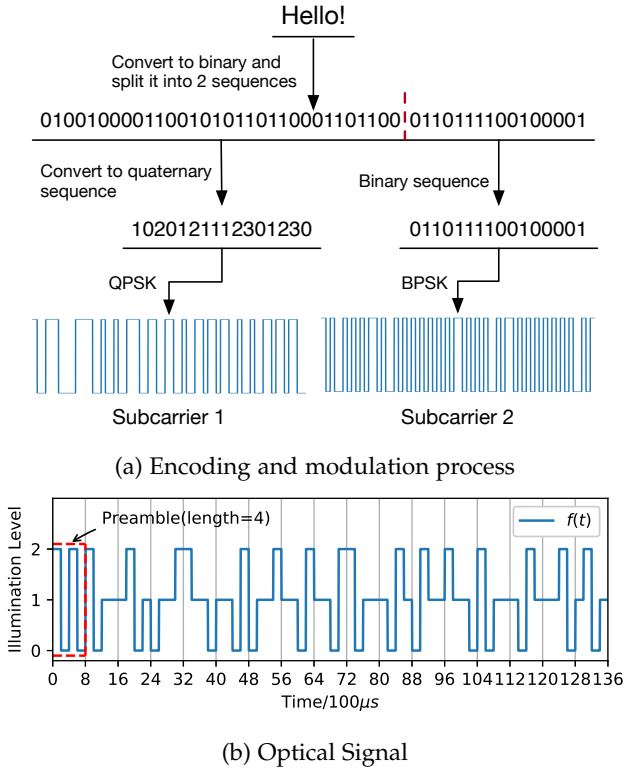


Fig. 7: An HYCACO encoding and modulation example which uses two LEDs to send the message *Hello!*.

- $i \leq T/2$ .
- $T/i \in \mathbb{N}$ .

Let  $\mathbb{I}$  denote the set of subcarrier subscript  $i$ , and  $\mathbb{D}$  denote the set of divisors of  $T$ . we can derive that  $\mathbb{I} \subseteq \mathbb{D} - \{T\}$ . Let  $I$  denote the number of LEDs, and  $I = |\mathbb{I}|$ . The proper  $T$  is

$$\min T \quad \text{s.t.} \quad |\mathbb{D} - \{T\}| \geq I. \quad (7)$$

Secondly, we encode the input data to N-ary symbols. The encoding scheme is as follows:

- 1) Convert the input data to binary.
- 2) Divide the binary sequence into  $I$  sequences, each of which is length of a multiple of  $\log_2(T/i)$ .
- 3) Convert the divided sequences to N-ary sequences correspondingly, where  $N = T/i$ .

Lastly, we distribute these N-ary sequences to the corresponding LEDs.

Let us use an example to demonstrate the encoding and modulation process. As illustrated in Fig. 7a, we use two LEDs to send the message *Hello!*. The modulated optical signal is shown in Fig. 7b.

## 4.2 Signal Recovery

A NLoS link typically has a low signal-to-noise ratio (SNR) because of the complex image background and the reflection. We tackle these challenges by taking a long exposure image which has the same EV as that of the short exposure images. EV is a number that represents a combination of a camera's exposure duration, ISO and f-number. Images captured with the same EV will present the same scene luminance [11]. For the f-number is fixed in smartphones,

the short and the long have the same depth of field. Thus, if the long is motion blur-free, they have the same texture layer, too. As illustrated in Fig. 8, the texture layer may not look the same in the two images. It's because the short is captured with a high ISO and thus introduces more image noise. The noise can be eliminated by the summation.

When  $t_e \gg t_i$ , the signal layer is approximately constant, and the long exposure image can be approximated as its texture layer [6]. Let  $i_{short}(y)$ ,  $i_{long}(y)$  and  $g(y)$  denote the short exposure image, the long exposure image and the signal layer of the short, respectively. Thus, according to equation (4),

$$g(y) = \frac{i_{short}(y)}{i_{long}(y)}. \quad (8)$$

The long exposure image only needs to be captured once at the beginning of the reception. As long as the communication time is long enough, the extra cost of capturing the long exposure image could be negligible.

The LEDs are located at different locations and have different distances and irradiance/incidence angles to the reflector. The channel gain of each LED-reflector link is different. The channel attenuations can be compensated by detecting the frequencies of the subcarriers. The compensation algorithm will be addressed in our future work. Here, we just assume the LEDs are adjacent. Thus, the channel gains are approximately equal. Equation (1) can be written as

$$e(t) = K f(t) + E, \quad (9)$$

where  $K = H(0)L$ . Non-flickering component  $E$  can be filter out by a DC filter, as illustrated in Fig. 8.

We extract the packets by detecting the preambles in the signal layer. The transmitter sends a known preamble at the beginning of a packet, as shown in Fig. 7b. In the signal layer, the preamble is convolved with the shutter function to form one and a half cycles of a triangle wave, which starts at a peak. The extracted signal layer of the example in Section 4.1 is illustrated in Fig. 8. The preamble also gives us the information of the sampling period. Let  $n_p$  denote the width of the preamble in the signal layer. The width proportional to one unit time in the signal layer is  $n_p/3$ , denoted by  $n_i$ .  $n_i$  can be used to estimate the readout duration  $t_r$ , i.e.,  $t_r = t_i/n_i$ . We use  $n_i$  as the sampling period. Then, we normalize the sampling result to get an illumination level sequence, denoted by  $g[k]$ , as illustrated in Fig. 8. According to Nyquist-Shannon sampling theorem,  $g[k]$  can fully describe  $f(t)$ .

## 4.3 Demodulation and Decoding

We propose a superimposed square wave division algorithm to divide the optical signal into a set of square waveforms. The Fourier series of Equation (6) is

$$f_i(t) = \frac{1}{2} + \frac{2}{\pi} \sum_{n=1}^{\infty} \frac{\sin(i(2n-1)t + \theta)}{2n-1}, \quad (10)$$

where  $t \in [0, T)$ . The first sinusoid component ( $n = 1$ ) has the same frequency and phase as the square waveform.

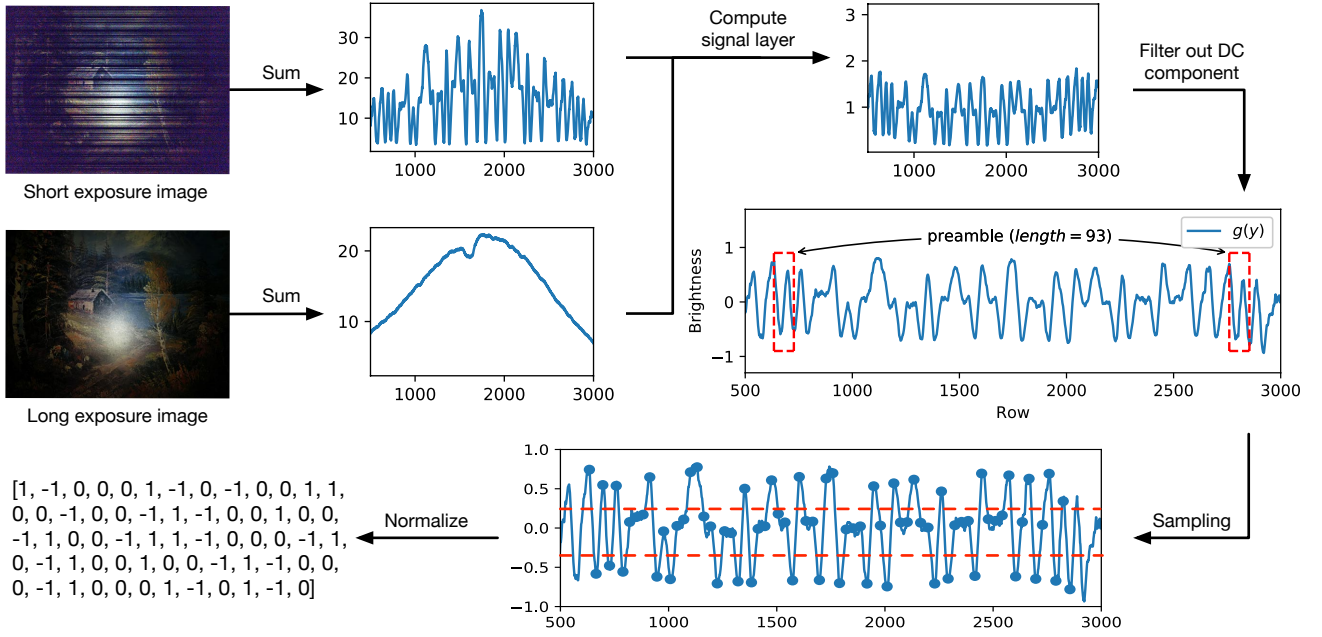


Fig. 8: Shows the process of signal recovery. The long exposure image has the same EV as the short one's. The results are a sequence which represents the illumination levels.

#### Algorithm 1 Superimposed Rect-wave Division (SURD)

**Input:**  $g[k], \mathbb{I}$   
**Output:**  $S[i]$   
 $\mathbb{X} \leftarrow$  short-time Fourier transform (STFT) of  $g[k]$   
**for each**  $X \in \mathbb{X}$  **do**  
  **for each**  $i \in \mathbb{I}$  **do**  
    **if**  $i = 1$  **then**  
       $X_i[i] \leftarrow X[i]$   
    **else**  
       $X_i[i] \leftarrow X[i] - \sum_{j=1}^{i-1, j \in \mathbb{I}} X_j[i]$   
    **end if**  
     $S[i] \leftarrow \frac{\angle X_i[i] \times T}{2i\pi}$   
    Calculate  $x_i$  via Equation (11)  
     $X_i \leftarrow$  Real DFT of  $x_i$   
  **end for**  
**end for**

When the continuous function  $f_i(t)$  is sampled at the inverse of one unit time Hz, we get the discrete form of  $f_i(t)$ ,

$$x_i[k] = \frac{1}{2} + \frac{2}{\pi} \sum_{n=1}^{T/2i} \frac{\sin\left(i(2n-1)2\pi\left(\frac{k+S_i}{T}\right)\right)}{2n-1}, \quad (11)$$

where  $k = 0, 1, 2, \dots, T-1$ . Thus, the discrete form of the optical carrier is  $x[k] = \sum x_i[k]$ . By taking a real discrete Fourier transform (DFT) of both sides, we get the frequency domain,

$$X[\omega] = \sum X_i[\omega], \quad i \in \mathbb{I}, \quad (12)$$

where  $\omega = 0, 1, 2, \dots, T/2$ .  $\angle X_i[i]$  is the phase of the  $i^{\text{th}}$  subcarrier. The frequency bins  $X_i[\omega]$  represent the sinusoid components which construct the subcarrier  $x_i$ , where  $\omega$  is the frequency of the sinusoid component. We can see that  $X_i[\omega] = 0$  when  $\omega \neq i(2n-1)$  and  $\omega \neq 0$ , hence  $X_1[1] =$

$X[1]$ . The demodulation process is expressed in Algorithm 1.

#### 4.4 Dealing with Unsynchronized Communications

We address the symbol loss problem with LT codes. LT codes employ a particularly simple algorithm based on the XOR to encode and decode the message. We encode the input data to LT codes before the HYCACO encoding process. The process of generating an encoding packet is easy to describe:

- 1) Divide the input data into  $n$  blocks of roughly equal length.
- 2) Randomly choose  $d$  blocks, where  $1 \leq d \leq n$  and the degree  $d$  is a pseudorandom number.
- 3) The value of the encoding symbols is the XOR of the  $d$  blocks, i.e.,  $M_{i_1} \oplus M_{i_2} \oplus \dots \oplus M_{i_d}$ , where  $M_i$  is the  $i^{\text{th}}$  packet and  $\{i_1, i_2, \dots, i_d\}$  are randomly chosen indices of the  $d$  blocks.
- 4) A prefix is appended to the symbols defining the list of indices and the total blocks  $n$  in the input data.

We perform the HYCACO encoding and modulation process on these encoded packets. The receiver keeps extracting packets from the captured images. If a packet is of degree  $d > 1$ , it is first XORed against all the decoded packets in a message queuing area, then stored in a buffer area if its reduced degree is greater than 1. When a new packet of degree  $d = 1$  is received or reduced, it is moved to the message queuing area and matched against all the packets in the buffer. When all  $n$  packets have been moved to the queuing area, the received data has been successfully decoded.

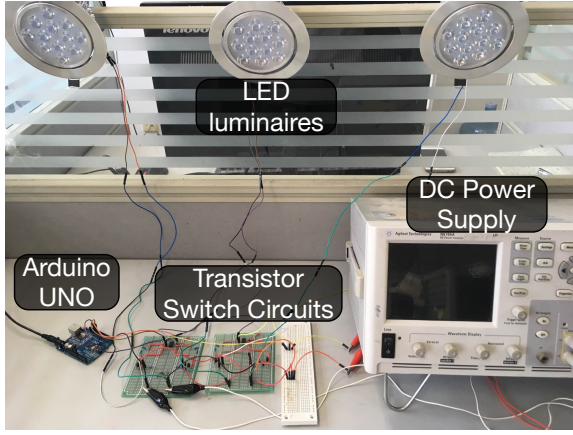


Fig. 9: Experimental equipments of the transmitter

## 5 EVALUATION

### 5.1 Experiment Setup

The transmitter of our hardware prototype for HYCACO consists of a DC power supply, an Arduino UNO, 3 transistors switch circuit boards and 3 COTS LEDs (shown in Fig. 9). The transistor switch circuit boards are used to amplify the signal to a proper voltage level for the LEDs. The circuit boards are connected to the Arduino UNO, the microcontroller, which accepts the input data and generates *ON-OFF* symbols. On the receiver side, we test two devices, iPhone 6s and Nexus 5. We check the performance of throughput for various settings, such as dimensions, exposure duration, packet size and frame rate.

### 5.2 Achievable Throughput

#### *Impact of the number of LEDs*

According to Equation (7), the more LEDs in HYCACO modulation scheme, the longer duration the transmitter needs to send a symbol. Therefore, the number of LEDs determines the symbol duration, the symbol duration determines the granularity of packets, and different levels of granularity cause different symbol loss ratios. We set the time unit as  $100 \mu s$ . Assuming that no symbol is lost, the frame throughputs of using different numbers of LEDs for transmission are illustrated in Fig. 10a. We can see that HYCACO reaches the highest frame throughput when the number of LEDs is 5,  $T = 12$ , and  $\mathbb{I} = \{1, 2, 3, 4, 6\}$ . The frame throughput of using Nexus 5 is higher than that of using iPhone 6s, although images captured by iPhone 6s have larger dimensions. This is because the readout duration of iPhone 6s is much smaller than that of Nexus 5. According to our experiments, the readout duration of iPhone 6s and Nexus 5 are  $6.45 \mu s$  and  $12.5 \mu s$ , respectively.

#### *Impact of the packet size*

However, we need a preamble preceding each packet to extract the packets from the signal layer. The preamble takes an extra cost of 4 units time for the transmitter to send a packet. Signals before the first detected preamble and after the last detected preamble are discarded. As shown in Fig. 10b, the number of symbols in a packet affects the frame throughput. We use iPhone 6s to capture images with

dimensions of  $3024 \times 4032$ . If the packet size is small, the preambles take more shares in the signal layer, while the packet size is big, the discarded signals might be big, too.

#### *Impact of the frame rate*

We check the impact of the camera frame rate on the throughput. iPhone 6s supports to capture images at higher frame rates up to 240 fps but with lower resolutions. The test results are illustrated in Fig. 10c. The throughput reaches the maximum when the frames are captured in 3024p/30 format.

## 5.3 Realistic Performance

In this section, we conduct our evaluations based on the following metrics:

- *Throughput*: the average amount of data successfully decoded per second in the received frames.
- *Bit error rate (BER)*: the percentage of wrongly decoded data in the total amount of data.
- *Overall error rate*: the percentage of overall detection error, including the frames failed to extract, the packets failed to demodulate, and the wrongly decoded bits. This can be expressed as  $p_e = 1 - p_f \times p_p \times p_b$ , where  $p_f$ ,  $p_p$  and  $p_b$  are the percentage of successfully decoded frames, packets and bits, respectively.

We examine the realistic performance under various environments with different exposure durations. According to the test results in Section 5.2, we choose  $I = 3$  and  $N = 4$ , i.e., the transmitter consists of 3 LEDs and the number of HPSK symbols per packet is 4. We use iPhone 6s as the receiver. The dimensions of the camera are set to  $3024 \times 4032$ , and the frame rate is 30 fps. We put a lumen meter at a fixed location, and the measured ambient illumination is 200 lux.

#### *Impact of the distance and angle*

We first check the impact of the distance and the viewing angle between the camera and the reflector. The measured illuminance is 450 lux. The test results are illustrated in Fig. 11a, 11b, 11c, 11d, 11e and 11f, respectively. The results show that the distance and angle have next to no impact on the performance when the exposure duration is larger than  $100 \mu s$ . This is very different from the LoS LCC approaches, which are highly affected by the distance and angle. We find the distance and the angle affect the performance when the exposure duration is set to  $50 \mu s$ .

#### *Impact of the illuminance*

We change the luminance of the LED by adjusting the supply voltage. The LED we use supports a voltage ranging from 25 V to 40V. We put the camera parallel to the reflector at a fixed location. As shown in Fig. 11g, 11h and 11i, the luminance has different impacts on the performances of different exposure durations. The overall error rate increases when the illuminance is smaller than a threshold. The threshold increases with the increase of the exposure duration.

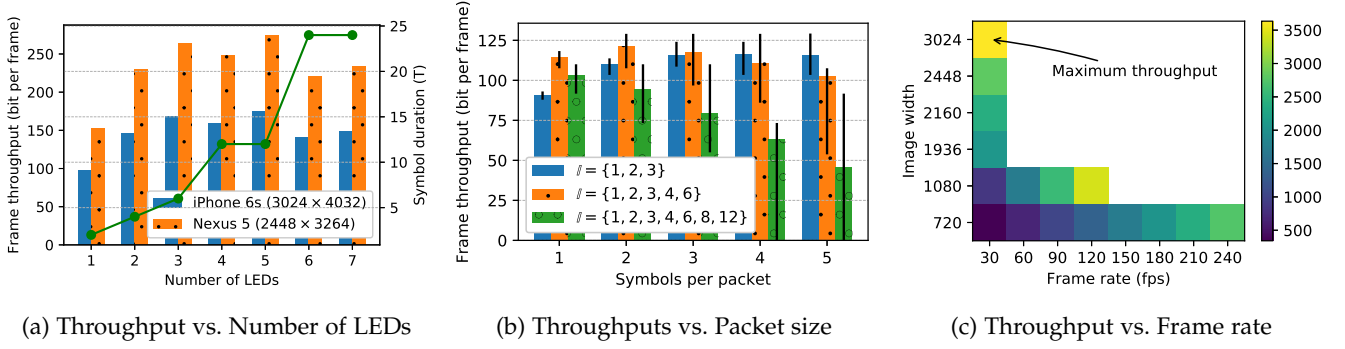


Fig. 10: The ideal achievable throughput. *Frame throughput* is the amount of data decoded per frame.

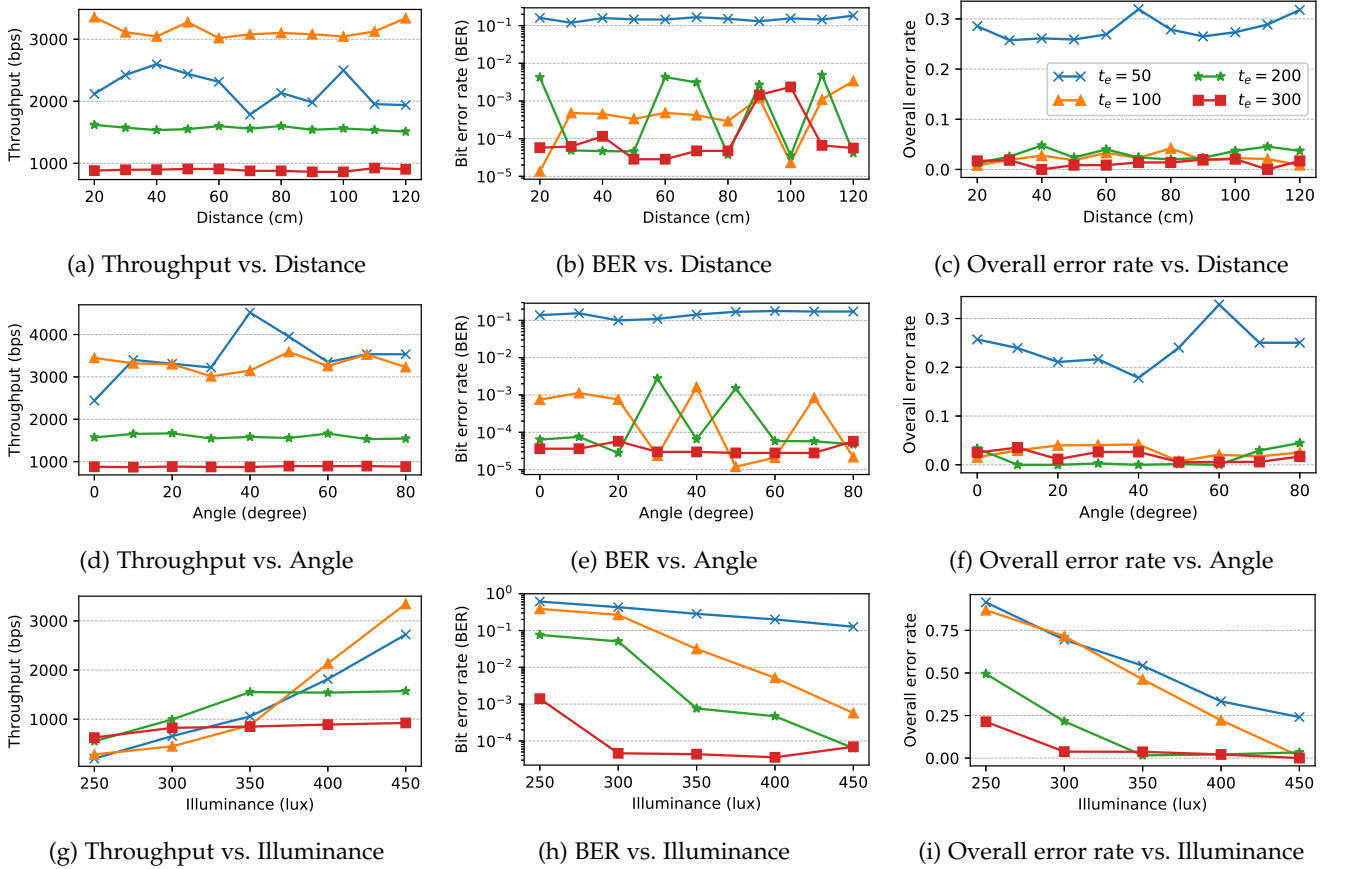


Fig. 11: The impacts of distance, angle, illuminance and exposure duration on throughput, BER and overall error rate, respectively. The transmitter-reflector distances are fixed. The lumen meter is put at a fixed location.

### Impact of the exposure duration

We check the performance of different exposure durations. The test range of the exposure duration is from 50 to 300  $\mu$ s. When the exposure duration is larger than 300  $\mu$ s, the symbol duration is too long that the receiver could only capture one packet per frame. The test results are illustrated in Fig. 11. We can see the throughput increases with the decrease of the exposure duration. However, when the exposure duration and/or the illuminance is smaller than a threshold, the BER and the overall error rate will increase. We find when the illuminance is higher than 450 lux and the exposure duration is larger than 100  $\mu$ s, the frames are decoded with a BER lower than 1% and an overall error rate

lower than 5%.

## 6 DISCUSSION

Cameras on the market usually have different frame rates, dimensions, and readout durations. The throughputs of LCC systems are highly related to these features. Moreover, LCC is unsuitable for continuous receptions due to its high power consumption. Therefore, the first aim of an LCC system should be easy to use rather than the high throughput. The application scenarios of LoS LCC are restricted by the small RoI and the field-of-view (FoV) of the camera. Light suffers less from multipath effects than WiFi signals, and

the radiant intensities follow an attenuation pattern. NLoS LCC can be used for indoor positioning and/or orientation techniques by estimating the channel gain of the transmitter-reflector links. We plan it for future work.

Our prototype works fine under a condition that the illuminance perceived by the camera is proportional to the number of the ON-state LEDs. Employing more LED luminaires for transmission may violate the assumption. The relative position of the camera and the reflector has nearly no impact on the performance, because the channel gain of the reflector-camera link is the same for all transmitters. Whereby the perceived illuminance differences are dominated by the transmitter-reflector links. When HYCACO can work with channel compensations, the application scenarios will be various.

## 7 RELATED WORK

**NLoS LCC.** Most of the existing NLoS LCC approaches only utilize one LED for transmission. Danakis et al. [12] first propose that the CMOS camera can be used as a receiver in order to capture the continuous changes of the status (ON-OFF) of the light. MILC [13] improves the throughput with multi-level illuminations. Martian [2] encodes bits by varying the duty cycle of a pulse waveform. Rajagopal et al. [14] propose a hybrid VLC system, which simultaneously transmits low-speed data to cameras and high-speed data to photodiode receivers. ReflexCode [3] adopts reflected light emitted from multiple LEDs as its communication media. It is actually another way to implement multi-level illuminations, and the LEDs need to be adjacent to each other. Using a single LED to provide multi-level illuminations need an additional hardware like a DAC, which will increase the cost. Varying the luminous intensity or the duty cycle may break the overall brightness energy balance. The LEDs in HYCACO flicker with a constant duty cycle (50%) and thus are naturally flicker-free to human eyes.

**LoS LCC.** If an LCC has sufficient brightness, the LoS link has a sufficient SNR and thus is more resilient to the ambient noise. RollingLight [1] employs frequency shift keying scheme and delivers a throughput of 11.32 Bps. However, this throughput is achieved when the camera is very close to the LED. CamCom [15] uses undersampled frequency shift OOK to encode bits, and it achieves a throughput of 400 bps using 100 LEDs. Luo et al. [16] propose undersampled phase shift OOK, and their system reaches 150 bps with a dual LED lamp. The major bottleneck of throughput is the small RoI. Besides, LoS LCC provides a natural way to enable visual association, which creates an opportunity for indoor positioning. Luxapose [17] explores the indoor positioning problem by detecting the presence of the luminaires in the captured image. LiTell [18] proposes a robust localization scheme that employs unmodified fluorescent lights (FLs) as location landmarks. However, these positioning schemes need LoS links and enough spatial resolutions to separate transmissions from different transmitters.

**Other Recent VLC Works.** Several recent works investigate other specific types of VLC. Screen-to-camera communications [7], [19], [20] employ the screens as the transmitters which have larger dimensions and more changing states. Disco [6] uses a modified display as the transmitter to send

sine wave signals. It recovers the signals with a simultaneous dual exposure (SDE) sensor. DarkLight [21] allows light-based communication to be sustained even when the LED lights appear dark or OFF. ColorBars [22] utilizes Color Shift Keying (CSK) to modulate data using different colors transmitted by the LED. Kaleido [8] utilizes the rolling shutter effect to prevent unauthorized users from taping a video played on a screen. LCC is a just a special type of VLC. In the transmitter, the rolling shutter deforms the signal frequency spatial detail by convolution. Thereby, with the proposed signal recovery approach, lots of modulation schemes employed in other kinds of VLC systems can also be employed in LCC.

## 8 CONCLUSION

In this paper, we design and implement HYCACO, which enables multiple access for NLoS LCC. We demonstrated the efficacy of our design using a hardware prototype, which achieves a throughput of 4.5 Kbps. HYCACO works fine when the measured illuminance is 450 lux which is the recommended illuminance for an indoor environment. Unlike the width-driven demodulation [1], [2], which is complex in computation, we just sample hundreds of judging points from the received signal for the demodulation. Therefore, HYCACO is high computational efficiency and can provide realtime responses with hand-held devices. The major concern of NLoS links is the signal power attenuation. When we extract the signal layer from the short exposure image by dividing it from a long exposure image, not only the image background is eliminated, but also the SNR is enhanced. If we use the existing LED infrastructures for transmissions, the channel gains of the LED-reflector links will be different. We can add a compensation algorithm to make HYCACO functional or use the channel properties for indoor positioning. We plan to address these challenges in future work.

## REFERENCES

- [1] H.-Y. Lee, H.-M. Lin, Y.-L. Wei, H.-I. Wu, H.-M. Tsai, and K. C.-J. Lin, "Rollinglight: Enabling line-of-sight light-to-camera communications," in *Proceedings of the 13th Annual International Conference on Mobile Systems, Applications, and Services*. ACM, 2015, pp. 167–180.
- [2] H. Du, J. Han, Q. Huang, X. Jian, C. Bo, Y. Wang, H. Xu, and X. Li, "Martian—message broadcast via led lights to heterogeneous smartphones: poster," in *Proceedings of the 22nd Annual International Conference on Mobile Computing and Networking*. ACM, 2016, pp. 417–418.
- [3] Y. Yang, J. Nie, and J. Luo, "Reflexcode: Coding with superposed reflection light for led-camera communication," *Proc. of the 23th ACM MobiCom (to appear)*, 2017.
- [4] M. Luby, "Lt codes," in *Foundations of Computer Science, 2002. Proceedings. The 43rd Annual IEEE Symposium on*. IEEE, 2002.
- [5] J. M. Kahn and J. R. Barry, "Wireless infrared communications," *Proceedings of the IEEE*, vol. 85, no. 2, pp. 265–298, 1997.
- [6] K. Jo, M. Gupta, and S. K. Nayar, "Disco: Display-camera communication using rolling shutter sensors," *ACM Transactions on Graphics (TOG)*, vol. 35, no. 5, p. 150, 2016.
- [7] W. Hu, H. Gu, and Q. Pu, "Lightsync: unsynchronized visual communication over screen-camera links," in *Proceedings of the 19th annual international conference on Mobile computing & networking*. ACM, 2013, pp. 15–26.
- [8] L. Zhang, C. Bo, J. Hou, X.-Y. Li, Y. Wang, K. Liu, and Y. Liu, "Kaleido: You can watch it but cannot record it," in *Proceedings of the 21st Annual International Conference on Mobile Computing and Networking*. ACM, 2015, pp. 372–385.

- [9] J. Gancarz, H. Elgala, and T. D. Little, "Impact of lighting requirements on vlc systems," *IEEE Communications Magazine*, vol. 51, no. 12, pp. 34–41, 2013.
- [10] S. Keeping, "Characterizing and minimizing led flicker in lighting applications," *Electronic Products magazine*, 2012.
- [11] D. Wüller and H. Gabele, "The usage of digital cameras as luminance meters." in *Digital Photography*, 2007, p. 65020U.
- [12] C. Danakis, M. Afgani, G. Povey, I. Underwood, and H. Haas, "Using a cmos camera sensor for visible light communication," in *2012 IEEE Globecom Workshops*. IEEE, 2012, pp. 1244–1248.
- [13] Z. Yang, H. Zhao, Y. Pan, C. Xu, and S. Li, "Magnitude matters: A new light-to-camera communication system with multilevel illumination," in *Computer Communications Workshops (INFOCOM WKSHPS), 2016 IEEE Conference on*. IEEE, 2016, pp. 1075–1076.
- [14] N. Rajagopal, P. Lazik, and A. Rowe, "Hybrid visible light communication for cameras and low-power embedded devices," in *Proceedings of the 1st ACM MobiCom workshop on Visible light communication systems*. ACM, 2014, pp. 33–38.
- [15] R. D. Roberts, "Space-time forward error correction for dimmable undersampled frequency shift on-off keying camera communications (camcom)," in *Ubiquitous and Future Networks (ICUFN), 2013 Fifth International Conference on*. IEEE, 2013, pp. 459–464.
- [16] P. Luo, Z. Ghassemlooy, H. Le Minh, X. Tang, and H.-M. Tsai, "Undersampled phase shift on-off keying for camera communication," in *Wireless Communications and Signal Processing (WCSP), 2014 Sixth International Conference on*. IEEE, 2014, pp. 1–6.
- [17] Y.-S. Kuo, P. Pannuto, K.-J. Hsiao, and P. Dutta, "Luxapose: Indoor positioning with mobile phones and visible light," in *Proceedings of the 20th annual international conference on Mobile computing and networking*. ACM, 2014, pp. 447–458.
- [18] C. Zhang and X. Zhang, "Litell: robust indoor localization using unmodified light fixtures," in *Proceedings of the 22nd Annual International Conference on Mobile Computing and Networking*. ACM, 2016, pp. 230–242.
- [19] W. Du, J. C. Liando, and M. Li, "Softlight: Adaptive visible light communication over screen-camera links," in *Computer Communications, IEEE INFOCOM 2016-The 35th Annual IEEE International Conference on*. IEEE, 2016, pp. 1–9.
- [20] B. Zhang, K. Ren, G. Xing, X. Fu, and C. Wang, "Sbvlc: Secure barcode-based visible light communication for smartphones," *IEEE Transactions on Mobile Computing*, vol. 15, no. 2, pp. 432–446, 2016.
- [21] Z. Tian, K. Wright, and X. Zhou, "The darklight rises: Visible light communication in the dark," in *Proceedings of the 22nd Annual International Conference on Mobile Computing and Networking*. ACM, 2016, pp. 2–15.
- [22] P. Hu, P. H. Pathak, X. Feng, H. Fu, and P. Mohapatra, "Colorbars: Increasing data rate of led-to-camera communication using color shift keying," in *Proceedings of the 11th ACM Conference on Emerging Networking Experiments and Technologies*. ACM, 2015, p. 12.